Coupling of in-line UVPPD rheometry and USDMA for process control in polymorph crystallization processing of chocolate confectionery masses

Erich Windhab[1], Kim Mishra[2], and Lucas Grob[3]

[1] Lab of Food Process Engineering (FPE/IFNH); ETH Zürich, Schmelzbergstrasse 9; CH-8092 Zürich
[2] Planted Foods AG; Kemptpark 32-34, CH-8310 Kemptthal; Switzerland
[3] Swiss Food Research; Schmelzbergstrasse 9; CH-8092 Zürich

The Ultrasound Velocity Profile Pressure Difference (UVPPD) method has proved to be a powerful in-line measuring technique for non-invasive flow mapping and characterization of Non-Newtonian fluid rheology in processing flows. Crystal melt suspensions (CMS) are yield stress shear thinning fluids in which crystal network formation is responsible for the appearance of a yield stress. CMS were made from different confectionery fat systems. UVPPD measurements were applied to determine the yield stress τ_0, as indicator of crystal network formation during following processing steps: (1) pre-crystallization, (2) micro-foaming, (3) 3D-printing and (4) molding, cooling and de-molding, being key operations in the chocolate confectionery manufacture. The coupled application of Ultrasound Dynamic Mechanical Analysis (USDMA) based on ultrasound attenuation comes into preferable consideration when the material characteristics switches from concentrated crystal suspension to a solid to detect fat crystal network formation during solidification. This was addressed for 3D-printed and molded chocolate masses upon cooling. With an ETH-FPE developed in-line sensing USDMA setup (DETACHLOG) we managed to correlate viscous and elastic moduli (G'', G') with crystal network structure formation. Moreover, it was possible to sharply detect the impact of the molded mass contraction during solidification and its subsequent detachment from the mold walls.

Keywords: Keywords: Ultrasound-Doppler, Ultrasound Attenuation, in-line rheometry and dynamic mechanical analysis, mold wall detachment detection, process control for crystallization, foaming, 3D-Printing and cooling

1. Introduction

The flow behaviour and material characterization of yield stress fluids containing crystals play a major role in lipid (fat/oil), polymer, metal or magma melts as well as in concentrated dispersion systems. They have in common that a liquid (melt or solution) and solid (crystal) may coexist under given temperature conditions. From a rheological perspective, cooling a melt below its crystallization temperature or a solution below a temperature at which supersaturation reaches a critical value, crystal formation transforms the fluid system from a Newtonian fluid to a non-Newtonian suspension or a semisolid body. Rheology-structure relationships of crystallizing fluid systems are mostly quite complex since the crystal structure and formation kinetics can be altered by shear stress and related viscous friction-based energy dissipation acting in shear flow fields. Accordingly, thixotropy or rheopexy can be superimposed with related characteristic time scales depending on shear stress and energy dissipation rates as well as on the generated crystal shape and morphology. Such complex relationships are often poorly understood despite their relevance in applications of lipid, polymer or metal, melt flow. Theoretical and experimental studies investigating lipid melt rheology were found to resemble each other. Recently, efforts have been made to introduce gas bubbles into lipid systems. Such systems are denoted as lipid foams. Most studies of such relate foam formation of lipid systems to the presence of crystals. Several stabilization mechanisms are proposed such as pickering stabilization, viscoelastic gel formation of the continuous phase, and jamming of crystals between bubbles. Confectionery fats are natural mixtures of high melting and low melting triglycerides. Micro-foaming of chocolate confectionery has become a novel and interesting developing domain aiming for a new class of low energy density chocolate confectionery [1,2]. This requires improved characterization of confectionery fat crystal structure formation and the development of related rheological and mechanical properties during (i) pre-crystallization, (ii) micro-foaming, (iii) 3D-printing/molding and (iv) cooling processes, for which the ultrasound based UVPPD & USDMA were adapted and successfully tested. Industrial implementations are under development.

2. Experiments and modelling

2.1 In-line rheometry in crystallization process

The UVPPD measurements were done directly after pre-crystallization. Double mantled 15 mm pipes held at 27 °C were used to convey the crystal melt suspension. The pressure difference was measured in a 3.29 m pipe section. A diaphragm pressure sensor (CC1020, Labom GmbH, Hude, Germany) with a measurement range of 1.0−1.4 bar absolute pressure was used at the beginning of the pipe segment in order to calculate the pressure difference against atmospheric pressure at the pipe exit. In between the pressure sensor and the end of the pipe segment a custom, built polyvinyl chloride cell with inserted ultrasonic transducers was used to record the velocity profile. Two 4 MHz transducers (Imasonic SAS, France) with an active diameter of 5 mm were placed at 60° and 90° angle with respect to the flow axis in order to determine the velocity profile across the pipe diameter and the speed of sound consecutively. The transducers were preferably operated at 3.75 MHz with a pulse repetition frequency of 750 Hz and

128 repetitions. The signals of the transducers were recorded with the UB-Lab device (Ubertone, Schiltigheim, F). During approximately 60 s, a total of six averaged profiles were recorded for one process setting. This procedure was repeated three times for each process setting. Subsequently, the profiles were deconvoluted and fitted with a Herschel-Bulkley model [3-5]. Fitting the Herschel-Bulkley model onto the measured velocity profile requires pipe radius R, plug radius Rp, pipe length Lp, flow index n, and consistency factor K as parameters:

$$\nu_{HB}(r) = \begin{cases} \frac{n}{n+1}\frac{\Delta P}{2L_p K}^{1/n}\left[(R-R_p)^{1+1/n} - (r-R_p)^{1+1/n}\right], & \text{if } r \geq R_p \\ \nu_{HB}(R_p), & \text{if } r < R_p \end{cases} \quad (1)$$

The fitted plug radius Rp is related to the yield stress of the CMS as follows:

$$R_p = \frac{2\tau_0 L_p}{\Delta P} \quad (2)$$

Consequently, the larger Rp and ΔP, the higher the yield stress τ_0 of the CMS. The instrumentation diagram for the crystallization and micro-foam processing including the UVPPD in-line measuring cell can be seen in Figure 1.

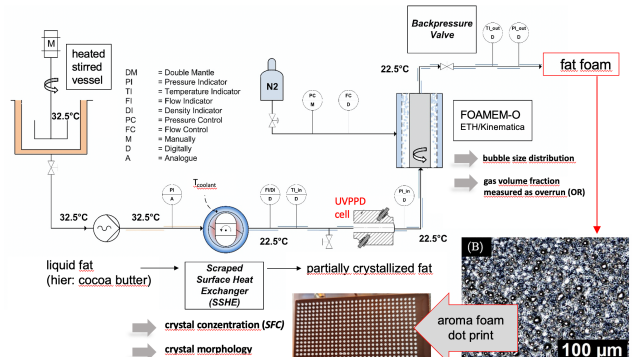

Figure 1: Processing setup for the processing of 3D-printed micro-foam structures from pre-crystallized fat crystal suspensions

Figure 2 shows further details of the UVPPD cell arrangement while Figure 3 demonstrates measured velocity profiles for various crystallization intensity and respectively derived yield values $\tau_{0,i}$.

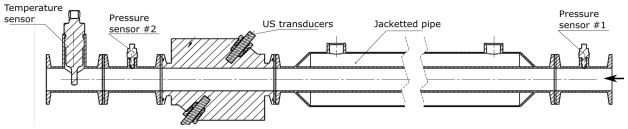

Figure 2: Arrangement of US and pressure transducers in the UVPPD measuring cell and p,T sensors in the related pipe section

The velocity profiles in Figure 3 were measured for cocoa butter melt suspensions (CB CMS) crystallized at apparent shear rates in the surface scraped heat exchanger of $\dot{\gamma}_{SSHE} = 2150\ s^{-1}$ for varying crystal volume fraction Φ_{SFC}. At low Φ_{SFC} an almost parabolic velocity profile is apparent. At $\Phi_{SFC} = 2.66$ % a center plug is forming indicating the onset of a yield stress. With further increasing Φ_{SFC} the plug flow domain extends further towards to the pipe wall. At $\Phi_{SFC} = 8.80$ %, the plug extends almost the whole pipe radius denoting the upper yield stress limit at the given measurement conditions.

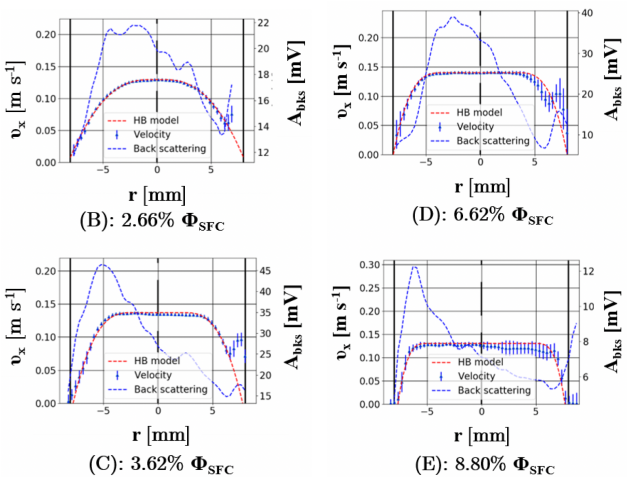

Figure 3: The fluid velocity in x-direction vx on the left y-axis and the back scattering amplitude $Abks$ on the right y-axis as function of the pipe radius r for CB CMS crystallized at $\gamma_{SSHE} = 2150\ s^{-1}$ for various crystal volume fractions ΦSFC. The lines emerging from the velocity profile points indicate the magnitude of uncertainty. The dotted red line indicates a fitted velocity profile according to the model proposed by Herschel and Bulkley.

Yield values as derived from the centre plug radii of the velocity profiles are presented in Figure 4 together with micrographs from polarized light microscopy of the resulting crystal structure.

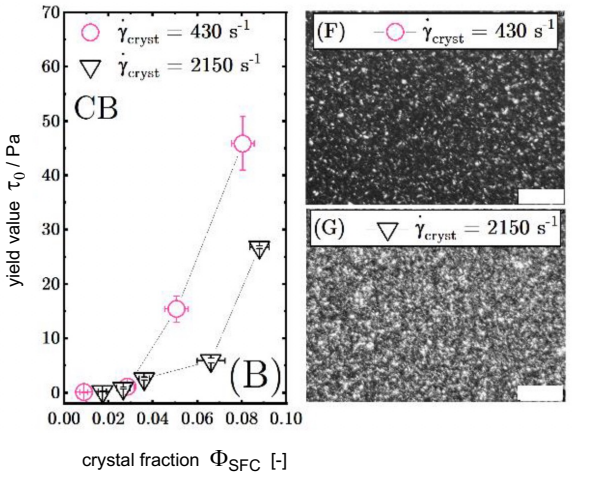

Figure 4: Left: Yield stress τ_0 as function of the crystal volume fraction Φ_{SFC} for CB, crystallized at $\dot{\gamma}_{SSHE} = 430\ s^{-1}$ & $2150\ s^{-1}$. (F,G) to the right displays of polarized light microscopy images of the respective CMS for both crystallization shear rates. Bar represents 100 µm [7].

As can be taken from Figure 4, crystallizing at increased shear rates leads to lower yield values in the CB system due to the generation of smaller crystals with reduced connectivity (network formation) expected to result from the increase viscous energy dissipation at higher shear rate. Yield stress τ_0 as a function of solid fat content Φ_{SFC} for

another fat melt system (palm kernel oil melt suspensions, PKO CMS) chosen as best reference fat base for chocolate confectionery fillings, was measured and resulting functional dependencies of $\tau_0(\Phi_{SFC})$ approximated with the structure model function given by equation 3:

$$\tau_0 = \frac{6\gamma}{a}\Phi^{1/(3-D)} \qquad (3)$$

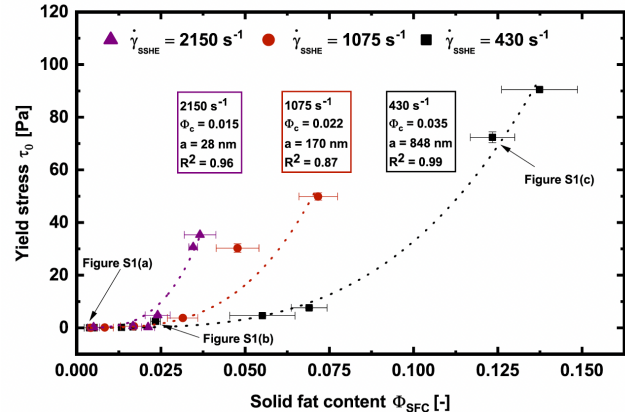

Figure 5. Yield stress τ_0 as a function of solid fat content Φ_{SFC} for PKO CMS crystallized at $\dot{\gamma}_{SSHE}$ = 430, 1075, and 2150 s^{-1}. The dashed lines indicate the fitted curves according to eq. 3 with the interfacial tension γ = 0.01 Nm^{-1} and the fractal dimension D = 2.7. The corresponding value of the primary particle diameter a, the critical crystal concentration Φc, and the resulting R^2 coefficient are displayed in the boxes.

2.2 Micro-foaming of fat crystal melt suspension

A membrane foaming apparatus (Kinematica Megatron MT-MM 1-52, Kinematica AG, Luzern, Switzerland) was used for the foaming of the CMS. The dynamically enhanced membrane foaming apparatus consists of two concentric cylinders [6]. The static outer cylinder with a diameter of 54.5 mm and an axial length of 60 mm acts as a membrane with nominal pore size of 3.5 µm. The inner rotating cylinder with a diameter of 44.5 mm generates a defined rheometric shear flow or a Taylor-Couette type of flow field depending on the fluid viscosity and the related Taylor number (Ta) in the 5 mm gap between the outer and inner cylinder thereby detaching the gas bubbles from the membrane surface and dispersing these into the continuous CMS phase. The CMS was axially pumped at 20 kg/h through the 5 mm gap of 60 mm length. Nitrogen gas was injected through the membrane into the gap at 7 bar with a flow rate of 20 L/h. A schematic radial cross-section of the foaming cell is depicted in the processing scheme in Fig 1.

Polarized light microscopy was used to investigate crystal morphology as well as bubble size distributions. Samples were slightly cooled during imaging by placing an ice container on the stage of the microscope. Gas bubble size and size distribution were calculated by using a custom-built image analysis software (ETH-SFP Bubble Detect). A minimum of 300 bubbles was counted to calculate a single bubble size distribution. SPAN values correspond to width divided by median bubble diameter of the distribution $(x_{90,0}-x_{10,0})/x_{50,0}$.

Previous work on membrane emulsification showed that the drop diameter is determined by the wall shear stress τ_w acting at the membrane surface and the pore diameter of the membrane. For the boundary condition $\tau_w > \tau_0$, the wall shear stress τ_w in the membrane foaming apparatus was calculated via the wall shear rate $\dot{\gamma}_w$ according to equations 4 and 5 given below for rotating inner cylinder and a static outer membrane cylinder.

$$\dot{\gamma}_w = \frac{2\Omega}{n((\alpha)^{2/n} - 1)} \qquad (7)$$

$$\tau_w = \tau_0 + K\dot{\gamma}_w^n = \tau_0 + \tau_{vs} \qquad (8)$$

The Bingham number Bm was introduced to describe the ratio of the yield stress τ_0 and the viscous flow stress τ_{vs} acting during gas bubble dispersion in the PKO CMS. The Bingham number Bm for a CMS in a shear flow is expressed as:

$$Bm = \frac{\tau_0}{\eta(\dot{\gamma}_w^n)\dot{\gamma}_w^n} = \frac{\frac{6\gamma}{a}\Phi^{1/(3-D)}}{K\dot{\gamma}_w^n} \qquad (9)$$

with the power law behavior of the structure-related yield value approximations considered.

Figure 6 demonstrate the functional relationship between the reciprocal Bingham number Bm^{-1} and the resulting normalized maximum bubble size $x_{90,0}$ of the foam generated under various solid fat content conditions at different shear rates in the membrane foaming device.

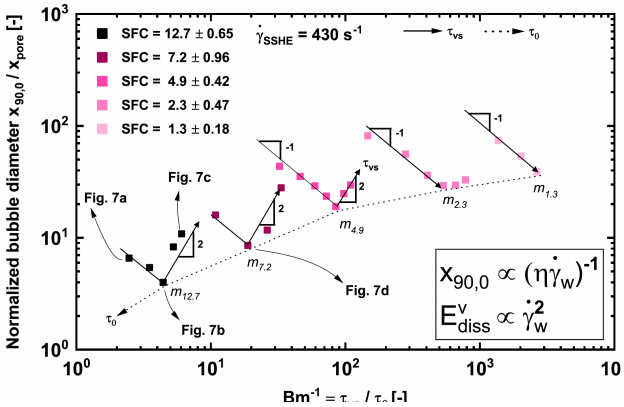

Figure 6. Normalized bubble diameter $x_{90,0}/x_{pore}$ as function of the reciprocal Bingham number Bm^{-1} for foamed PKO CMS crystallized at $\dot{\gamma}_{SSHE}$ of 430 s^{-1}. Direction of increasing viscous stress τ_{vs} for a given Φ_{SFC} is indicated (solid lines) as well as direction of increasing yield stress τ_0 (dashed line).

2.2 Novel 3D-printing of foamed fat suspensions

We introduced and applied a novel Additive Manufacturing (AM) approach capable of producing complex 3D food structures at elevated production rates and with added functionality. The complex 3D structure was broken down into three main length scales denoted as macro-, meso- and micro-scale. The macro-scale product elements acting as scaffold for the meso-scale elements were manufactured by twin-screw cold extrusion applying a macro-scale printing die (cm-range). Two six-axes robots equipped with a

single screw meso-scale (mm-range) extruder system and an electromagnetically triggered single/multi jetting micro-scale (100 mm scale) nozzle dose and shape the meso- & micro- scale product elements and connect them synchronously to the macro scale printed scaffold element. Figure 7 shows different views of the setup and product.

Figure 7: Setup for Multi-Scale Synchronous 3D-Printing of chocolate confectionery from foamed chocolate/fat crystal suspensions crystallized and foamed with in-line rheological control by UVPPD.

2.2 USDMA controlled solidification

The solidification under cooling conditions of micro-foamed and non-foamed chocolate confectionery is a final processing step being decisive for (1) shape retention of printed or molded products and for (2) the final formation of the fat crystal network concerning the crystal polymorph structure and the structure density. Both, (1) and (2) determine the final product structure significantly. The application of US attenuation measurements in order to detect fat crystal networking during solidification crystallization of molded chocolate masses during continuous cooling in industrial cooling tunnels has demonstrated to allow for viscosity and elasticity monitoring until the molded solidified product detaches from the mold wall or the 3D-printed product has solidified to an extent that it can be picked by robots and packaged. The degree of shrinkage of confectionery fat structure during its solidification is an important characteristic to enable proper demolding and improved resistance against fat migration and quality deterioration by fat bloom formation during storage. Figure 8 demonstrates the US-transmitter/receiver installation in a Makrolon mold and the characteristic US attenuation (US amplitude damping) pattern during chocolate mass solidification and final detachment from the mold wall. During solidification crystallization domains of initially (i) increasing viscosity and subsequent (ii) increasing elasticity upon crystal network formation were distinguished since increase in viscosity leads to increased US-amplitude damping, whereas elasticity increase causes a reduction of the damping effect.

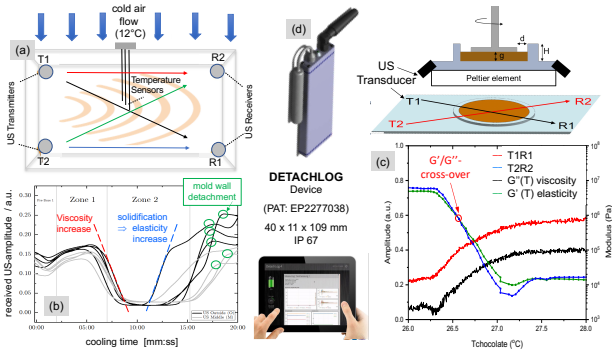

Figure 8: US-attenuation-based in-line measurement of molded chocolate during solidification & mold wall detachment (ETH-Detachlog) (a) US transmitter/receiver placement at mold bottom; (b) US-amplitude attenuation with differentiation of viscous /elastic contributions; (c) detailed analysis of viscous and elastic moduli (G'', G') during chocolate mass solidification [8].

3. Summary

The US-Doppler velocimetry based UVPPD technology was adapted for in-line measurements of the non-Newtonian rheological material functions of crystallized and micro-foamed chocolate confectionery fat crystal suspensions. The transient characteristics of such systems cannot be measured satisfyingly by off-line rheometry. For applications like foaming and 3D-printing the yield stress τ_0 was demonstrated to be the crucial rheological material parameter determining (i) fat crystal network formation, (ii) related stabilization of micro-foam bubble structure as well as (iii) contraction and structure density of the final product. As soon as the material behavior of the investigated confectionery/fat systems switch from paste-like to solid-like the introduced in-line USDMA (Ultrasound Dynamic Mechanical Analysis) based measurements allowed for monitoring solidification kinetics and structure density development. Thus, the applied US-based measuring principles are of pivotal relevance for application in chocolate confectionery industry. From such new insights optimization criteria for products and process design (crystallizer, 3D-Printer, cooling tunnel, foaming device, mold) are on the way to be developed and commercialized.

References

[1] K. Mishra et al. (2022) Journal of Colloid and Interface Science, vol. 630: no. Part A, pp. 731-741, Amsterdam: Elsevier, 2022.

[2] K. Mishra et al. (2021): Soft Matter, vol. 18: no. 6, pp. 1183-1193, Cambridge: Royal Society of Chemistry, 2021.

[3] Windhab, E. J (1995). Rheology in food processing, chapter 5, pp. 80–116. Springer US, Boston, MA, 1995.

[4] Ouriev, B., Windhab E. (2004); Measurement Science and Technology, 14(11):1963-1972, 2004.

[5] J Wiklund, B Birkhofer, S Jeelani, M Stading, E Windhab (2012); Appl. Rheol. 22 (2012) 42232

[6] Pokorny L., Kohler L., Takeda Y., Windhab E. (2016); Flow Measurement and Instrumentation; 52, pp.137-143

[7] K. Mishra, D. Dufour, E. Windhab (2020); Crystal Growth & Design, 20(2):1292–1301, 2020.

[8] E. Windhab et al. (2012); Patent Nr. EP2277038